3 October 1997

ELSEVIER

Chemical Physics Letters 277 (1997) 159–166

CHEMICAL PHYSICS LETTERS

Interplay of inhomogeneity and anharmonicity in 2D Raman spectroscopy of liquids

K. Okumura, Y. Tanimura

Division of Theoretical Studies, Institute for Molecular Science, Myodaiji, Okazaki, Aichi 444, Japan

Received 16 June 1997; in final form 30 June 1997

Abstract

Molecular vibrational modes of liquids are studied using the multi-mode Brownian motion model. We examine the effects of inhomogeneity on anharmonic contribution to the 2D Raman spectroscopy. We consider three types of inhomogeneous distribution of local oscillators and present analytical expressions for the 2D signal where the lowest-order anharmonicity is taken into account. Numerical estimations of them in the case of a simple single-mode system clarify the effects of the inhomogeneity. A multi-mode system with anharmonicity and nonlinear polarizability is also studied and numerically compared with a recent experiment on CS_2, which suggests a minor role of the inhomogeneity in this substance.

1. Introduction

After the initial proposal [1], the fifth-order off-resonant experiment or two-dimensional (2D) Raman spectroscopy has received considerable attention. This 2D technique has been shown to be sensitive to heterogeneous dynamics in condensed phases [1]. This prediction has led to a number of experiments to investigate the low frequency intermolecular modes of liquid molecules such as CS_2 [2–9]. Recently, a novel heterodyne detection of 2D Raman spectroscopy has been carried out [10], and has made it possible to probe intramolecular modes through the fifth-order processes.

The original theory [1] as well as subsequent works [11,12] assumed that the vibrational modes of molecules are harmonic and roles of inhomogeneity were examined by assuming a spatial distribution of such harmonic modes. In our previous work [13,14], we demonstrated the sensitivity of this experiment to weak anharmonicity of the vibrational modes. In there, we assumed the homogeneous distribution of the vibrational modes for simplicity. In realistic situation, however, one can expect to observe the effects of inhomogeneous or heterogeneous distribution of vibrational modes in addition to the effects of anharmonicity. Such a heterogeneity is expected especially for fast dynamics, since, during the fast motion, the local structure of the environment is essentially fixed and the local property affects observables directly without randomization. In the present article, we study the interplay of anharmonicity and inhomogeneous distribution of the mode.

In Section 2, we present analytical results for a single mode, which are estimated numerically. In Section 3, we consider a bimodal system and take into account the effects of both anharmonicity of the potential and nonlinear coordinate dependence of polarizability at the same time, making allowance for inhomogeneous distribution of the mode parameters.

0009-2614/97/$17.00
PII S0009-2614(97)00832-4

The results are compared with the experimental data obtained by Tokmakoff and Fleming [9], which indicates a minor role of inhomogeneity in CS_2. Final section comments on possible future directions of the theory. Details of derivation can be found in our series of papers [13–17].

2. Single-mode case

We consider the effective Hamiltonian for a single-mode system, which is given by

$$H = H_m - \hat{\alpha} E(\boldsymbol{r},t)^2, \tag{2.1}$$

where

$$H_m = \frac{P^2}{2M} + \frac{M\Omega^2}{2} Q^2 + V(Q) + \sum_{i=1}^{N} \left[\frac{p_i^2}{2m_i} + \frac{m_i \omega_i^2}{2} \left(q_i - \frac{c_i Q}{m_i \omega_i} \right)^2 \right]. \tag{2.2}$$

Here, polarizability and anharmonicity are assumed to be

$$\hat{\alpha} = \alpha_0 + \alpha_1 Q + \frac{1}{2!}\alpha_2 Q^2 + \cdots, \tag{2.3}$$

and

$$V(Q) = \frac{1}{3!} g_3 Q^3 + \frac{1}{4!} g_4 Q^4 + \cdots. \tag{2.4}$$

This system can be completely characterized by the parameters associated with the mode Q,

$M, \Omega, \alpha_i, g_i,$

and those associated with the bath modes q_i,

$m_i, \omega_i, c_i.$

In the following we assume the Ohmic dissipation in which all the bath parameters (m_i, ω_i, c_i) are represented by the single parameter γ. This γ can be interpreted as the strength of damping, since the classical equation of motion in the Ohmic case is expressed as [17]

$$M\frac{\mathrm{d}^2 Q(t)}{\mathrm{d}t^2} + \gamma \frac{\mathrm{d}Q(t)}{\mathrm{d}t} + \frac{\mathrm{d}V(Q(t))}{\mathrm{d}Q(t)} = R(t), \tag{2.5}$$

where $R(t)$ is the fluctuating force.

Under the assumption of weak anharmonicity of potential and weak nonlinearity of polarizability, the fifth-order signal can be divided into two component — the anharmonic and nonlinear components [13]. Suppose that all the nonlinear parameters α_i in Eq. (2.3) and the anharmonic parameters g_j in Eq. (2.4) are proportional to a^i and g^{j-2} $(j \geq 3)$, respectively, where a and g are dimensionless small parameters. We can show [13] that, if a is much larger than g (but still less than unity), the nonlinear component (proportional to $\alpha_1^2 \alpha_2$) dominates the signal, while in the opposite case $(a \ll g)$ the anharmonic component (proportional to $\alpha_1^3 g_3$) governs it. We can also show [13] that even if g_3 and g_4 are the same size the term proportional to $\alpha_1^3 g_4$ vanishes and only the $\alpha_1^3 g_3$ term contributes to the anharmonic component. In this sense, the cubic anharmonicity g_3 is especially important in the fifth-order signal. (In the same way, we can show the $(n+1)$th-order anharmonicity g_{n+1} is important in the $(2n+1)$th-order experiment [14].)

In this section we focus on the anharmonic component to clearly exhibit the interplay of inhomogeneity and anharmonicity. Then the signal is given by

$$I^{(5)}(T_1,T_2) = |R^{\mathrm{AH}}(T_1,T_2)|^2. \tag{2.6}$$

An inhomogeneous distribution of the frequency and damping constant can be taken into account by including the distribution function $S(\gamma,\Omega)$:

$$R^{\mathrm{AH}}(T_1,T_2) = \int_0^\infty \mathrm{d}\Omega' \int_0^\infty \mathrm{d}\gamma'\, S(\Omega',\gamma')\, R^{\mathrm{AH}}_{\Omega'\gamma'}(T_1,T_2). \tag{2.7}$$

Here, the response function of the homogeneous system with the parameters (Ω',γ') is given by [13]

$$R^{\mathrm{AH}}_{\Omega'\gamma'}(T_1,T_2) = \left(\frac{i}{\hbar}\right)^2 \alpha_1^3 \left(-\frac{i}{\hbar} g_3\right) \int_{T_1}^{T_1+T_2} \mathrm{d}t\, D^{(-+)}_{\Omega'\gamma'} \times (T_1+T_2-t)\, D^{(-+)}_{\Omega'\gamma'}(t-T_1)\, D^{(-+)}_{\Omega'\gamma'}(t). \tag{2.8}$$

The propagator in the above can be expressed as

$$D^{(-+)}_{\Omega'\gamma'}(t) = \theta(t)\frac{4\hbar}{iM}\int_0^\infty \mathrm{d}\omega\, J(\omega,\Omega',\gamma')\sin\omega t, \tag{2.9}$$

where $\theta(t)$ is the Heaviside function (step function) and

$$J(\omega,\Omega',\gamma') = \frac{1}{2\pi}\frac{\omega\gamma'}{(\omega^2-\Omega'^2)^2+\omega^2\gamma'^2}. \quad (2.10)$$

We note here that the time integration in Eq. (2.8) can be carried out analytically as shown below.

In the following, we consider three cases of distribution $S(\Omega',\gamma')$.

1. Purely homogeneous distribution,

$$S(\Omega',\gamma') = \delta(\Omega'-\Omega)\,\delta(\gamma'-\gamma). \quad (2.11)$$

2. Gaussian frequency distribution (width σ),

$$S(\Omega',\gamma') = \delta(\gamma'-\gamma)\frac{e^{-(\Omega'-\Omega)^2/2\sigma^2}}{\sqrt{2\pi}\sigma}. \quad (2.12)$$

3. Purely inhomogeneous distribution,

$$S(\Omega',\gamma') = \lim_{\epsilon\to 0}\delta(\gamma'-\epsilon)\frac{2}{\pi}\frac{\Omega'^2\gamma}{(\Omega'^2-\Omega^2)^2+\Omega'^2\gamma^2}. \quad (2.13)$$

This purely inhomogeneous case was introduced in Ref. [1] so that the third-order signal in this case coincides with that in the purely homogenous case.

In the purely homogenous case, an analytical expression for the response function is given by [13]

$$R^{\mathrm{AH}}(T_1,T_2) = -\frac{\alpha_0^3}{\hbar^2}\tilde{a}_1^3\tilde{g}_3\Omega_0^4\big[F(T_1)-F(T_1+T_2)\big], \quad (2.14)$$

where

$$F(t) = \frac{1}{4\zeta^3}\sum_{i=1}^{4}(-1)^i\frac{e^{-\gamma(T_2+t)/2}}{\gamma^2/4+(\zeta a_i)^2} \times\left\{\frac{\gamma}{2}\sin\zeta(a_i t+b_i)+\zeta a_i\cos\zeta(a_i t+b_i)\right\}, \quad (2.15)$$

with

$$(a_1,a_2,a_3,a_4) = (1,-1,-3,-1) \quad (2.16)$$

and

$$(b_1,b_2,b_3,b_4) = (T_2,T_2,2T_1+T_2,2T_1+T_2). \quad (2.17)$$

We have used the dimensionless parameters

$$\tilde{g}_3 = \frac{g_3}{\hbar\Omega_0}\left(\frac{\hbar}{M\Omega_0}\right)^{3/2}, \quad (2.18)$$

and

$$\tilde{a}_1 = \frac{\alpha_1}{\alpha_0}\left(\frac{\hbar}{M\Omega_0}\right)^{1/2}, \quad (2.19)$$

where Ω_0 is the unit of frequency, which can be any value. We stress here that ζ introduced in the above, which is defined by

$$\zeta = \sqrt{\Omega^2-\gamma^2/4}, \quad (2.20)$$

can be an imaginary number in the overdamped case ($\Omega<\gamma/2$).

In the case of Gaussian frequency distribution, we have

$$R^{\mathrm{AH}}(T_1,T_2) = -\frac{\alpha_0^3}{\hbar^2}\tilde{a}_1^3\tilde{g}_3\Omega_0^4\int_0^\infty\frac{d\Omega'}{\sqrt{2\pi}\sigma}e^{-(\Omega'-\Omega)^2/2\sigma^2} \times\big[F_{\Omega'}(T_1)-F_{\Omega'}(T_1+T_2)\big], \quad (2.21)$$

where $F_{\Omega'}(t)$ is defined by Eq. (2.15) with ζ replaced by $\zeta' = \sqrt{\Omega'^2-\gamma^2/4}$. Note here that, since the factor Ω_0^4 emerged when we made $\alpha_1^3 g_3$ a dimensionless quantity by use of Eqs. (2.18) and (2.19), this Ω_0^4 should not be averaged over by the integral. Note also here that the expression of $F(t)$ given in Eq. (2.15) with ζ replaced by ζ' and thus the integrand in Eq. (2.21) are singular at $\Omega' = 0,\sqrt{2}\,\gamma/3$, and $\gamma/2$. However, these singularities of the integrand in Eq. (2.21) are fictitious and can be removed by subtracting an appropriate constant from the expression (2.15) without changing the value of $F_{\Omega'}(T_1)-F_{\Omega'}(T_1+T_2)$, which is done in numerical calculations below.

In the purely inhomogeneous case, the response function can be expressed as

$$R^{\mathrm{AH}}(T_1,T_2) = -\frac{\alpha_0^3}{\hbar^2}\tilde{a}_1^3\tilde{g}_3\Omega_0^4\big[G(T_1)-G(T_1+T_2)\big], \quad (2.22)$$

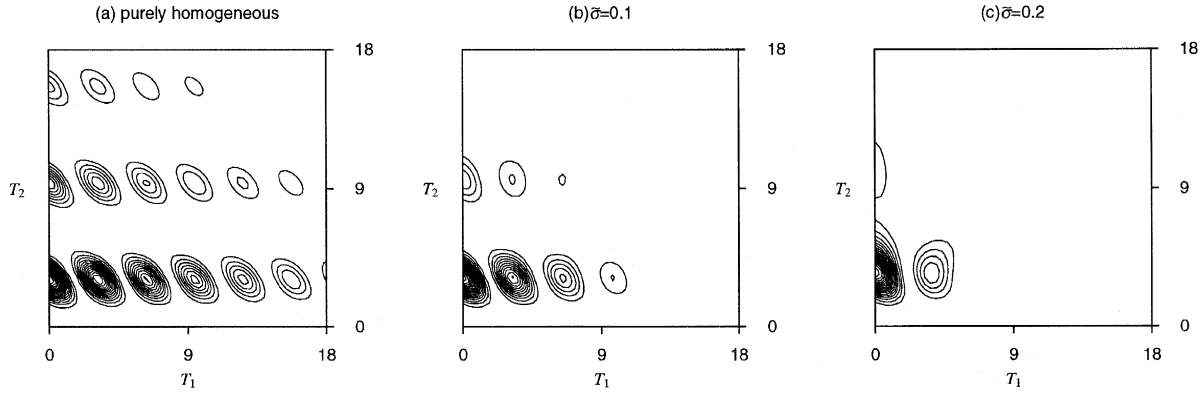

Fig. 1. Inhomogeneous effects for a weak damping mode. The width of Gaussian distribution of the frequency is increased from (a) to (c). The intensity of the signal $I^{(5)}$ is presented by contour plots.

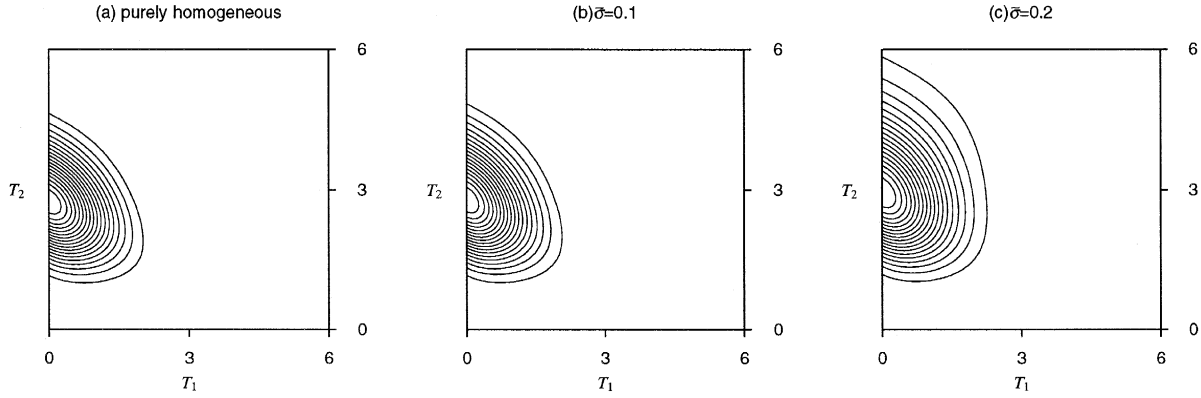

Fig. 2. Inhomogeneous effects for a strong damping mode. The width of Gaussian distribution of the frequency is increased from (a) to (c).

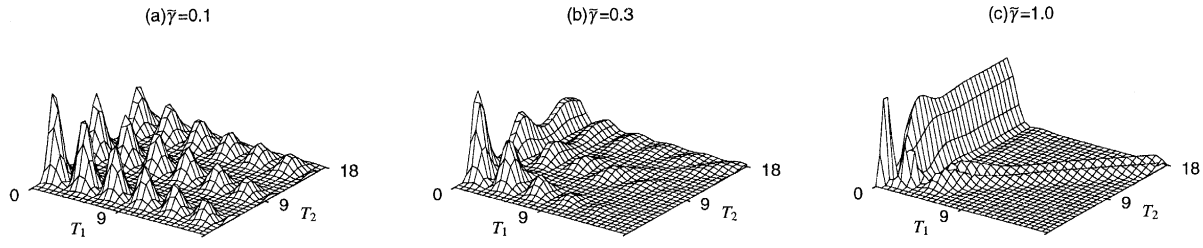

Fig. 3. Inhomogeneous effects in the purely inhomogeneous cases. The width of a distribution of the frequency of undamped oscillators are increased from (a) to (c). The intensity of the signal $I^{(5)}$ is presented by the three-dimensional plots.

where

$$G(t)=\frac{1}{4\zeta\Omega^4}\sum_{i=1}^{4}(-1)^i\frac{a_i\,\mathrm{e}^{-\gamma|a_it+b_i|/2}}{(\gamma a_i/2)^2+(\zeta a_i)^2}\times\Big\{\zeta(\Omega^2-\gamma^2)\cos\zeta(a_it+b_i)+\frac{\gamma}{2}(3\Omega^2-\gamma^2)\sin\zeta|a_it+b_i|\Big\},\qquad(2.23)$$

where a_i and b_i are the same as above and $|x|$ denotes the absolute value of x. In deriving this expression, we have used the relation,

$$\lim_{\epsilon\to 0}J(\omega,\Omega',\epsilon)=\frac{1}{4|\omega|}\big[\delta(\omega-\Omega')+\delta(\omega+\Omega')\big].\qquad(2.24)$$

Note here that, in the purely inhomogeneous case, an infinite number of *undamped* oscillators are distributed around the center frequency Ω with the width γ; the parameter γ is NOT the strength of the damping but the width of the inhomogeneous distribution [see Eq. (2.13)]. [1]

Numerical simulations for a single mode are presented in Figs. 1–3, where the unit of time is $1/\Omega$. In Figs. 1 and 2 we compare the purely homogeneous distribution and the Gaussian frequency distribution while in Fig. 3 we present the purely inhomogeneous cases.

In Fig. 1, we show results of numerical simulations for a weak damping ($\gamma/\Omega=0.1$). In (a) purely homogeneous case ($\sigma=0$), we see many oscillatory peaks since the coherence is maintained for a long period. The frequency of the oscillation along T_1 axis is Ω while that along T_2 is 2Ω. In (b) case of Gaussian frequency distribution with the width $\tilde{\sigma}\equiv\sigma/\Omega=0.1$, we observe less oscillatory peaks than in (a) since the distribution of the frequency implies destruction of the coherence. In (c) where $\tilde{\sigma}=0.2$, we see further less oscillations, which can be understood by the same reason.

In Fig. 2, we present results for a strong damping ($\gamma/\Omega=1.0$). In (a) purely homogeneous case, we see only one distinctive peak around $(T_1,T_2)=(0,3)$ since the coherent vibration is hidden due to the strong damping. In (b) case of Gaussian frequency distribution with the width $\tilde{\sigma}=0.1$, the peak is slightly more delocalized since many modes with different frequencies contribute to the signal. In (c) where $\tilde{\sigma}=0.2$, the peak is further delocalized by the same reason.

In Fig. 3, three cases of purely inhomogeneous distribution are compared. The parameter γ in these cases corresponds to the width of the frequency distribution as previously mentioned and the value of γ is increased from (a) to (c). In (a), since the distribution of frequencies is small, a coherent oscillation is observed. As we go from (a) to (c), we see that the time for which this coherence is maintained gets shorter because the frequency distribution gets larger. We note here that the two features in (c), the sharp ridge along the T_2 axis ($T_1\sim 0$) and the echo-like peak along the diagonal direction ($T_1=T_2$), had been observed in the result from the nonlinear components of the signal in the purely inhomogeneous case (see figure 6 of Ref. [1]).

3. Simulation for carbon disulfide

The experimental data by Tokmakoff and Fleming [9] can be modeled by the bimodal Hamiltonian [4,13]

$$H=H_L+H_H-\hat{\alpha}E(\boldsymbol{r},t)^2,\qquad(3.1)$$

where H_s ($s=L,H$) is defined through Eq. (2.2) where (M,Ω,γ,g_i) is replaced by $(M_s,\Omega_s,\gamma_s,g_{is})$. Here, the two modes ($Q_L$ and Q_H) are coupled through the polarizability

$$\hat{\alpha}=\alpha_0\exp\Big[\sum_{s=L,H}\tilde{a}_{1s}\tilde{Q}_s\Big],\qquad(3.2)$$

where $\tilde{Q}_s=Q_s\sqrt{M_s\Omega_0/\hbar}$.

Under the assumption of weak anharmonicity and weak nonlinear polarizability, the 2D signal in the purely homogeneous case is given by [13]

$$I^{(5)}(T_1,T_2)=|R^{\mathrm{AH}}(T_1,T_2)+R^{\mathrm{NL}}(T_1,T_2)|^2.\qquad(3.3)$$

The anharmonic contribution is expressed as

$$R^{\mathrm{AH}}(T_1,T_2)=\sum_{s=L,H}R_s^{\mathrm{AH}}(T_1,T_2),\qquad(3.4)$$

[1] Thus, the result in the purely homogeneous case at $\gamma=0$ and that in the purely inhomogeneous case at $\gamma=0$ should coincide with each other, which can be directly confirmed from Eqs. (2.15) and (2.23).

where $R_s^{\mathrm{AH}}(T_1,T_2)$ is given by Eq. (2.14) where $(\Omega, \gamma, \tilde{g}_3, \tilde{a}_1, \Omega_0)$ are replaced by $(\Omega_s,\gamma_s,\tilde{g}_{3s},\tilde{a}_{1s},\Omega_0)$. The nonlinear contribution is given by

$$R^{\mathrm{NL}}(T_1,T_2) = \frac{\alpha_0^3}{\hbar^2} f(T_2)\big[\, f(T_1+T_2) + f(T_1)\big], \tag{3.5}$$

where

$$f(t) = \sum_{s=L,H} \frac{\eta_s}{\zeta_s}\, \mathrm{e}^{-\gamma_s t/2} \sin\zeta_s t, \tag{3.6}$$

with $\zeta_s = \sqrt{\Omega_s^2 - \gamma_s^2/4}$ and $\eta_s = \Omega_0 \tilde{a}_{1s}^2$.

We can extract some of the parameters, almost uniquely, from the third-order experiment [4,13]: the set of parameters for the lower mode is $(\eta_L,\Omega_L,\gamma_L) = (1.00,12.9,43.0)$ and that for the higher mode is $(\eta_H,\Omega_H,\gamma_H) = (2.20,39.2,63.7)$ [cm^{-1}]. The remaining unspecified parameters are only $\tilde{g}_{3s}$, since $\tilde{a}_{1s}$ are already specified by η_s. In Ref. [13], we showed that the experimental data is similar to the results of numerical simulation if we assume $\tilde{g}_{3L} = 0$ and $\tilde{g}_{3H} = 0$ to $-6\tilde{a}_{1H}$. In the following, we consider this parameter region for numerical estimations.

The two modes in CS_2 can be associated with the fast librational motion (Ω_H) and the slow diffusive motion (Ω_L), respectively [13]. The diffusive dynam-

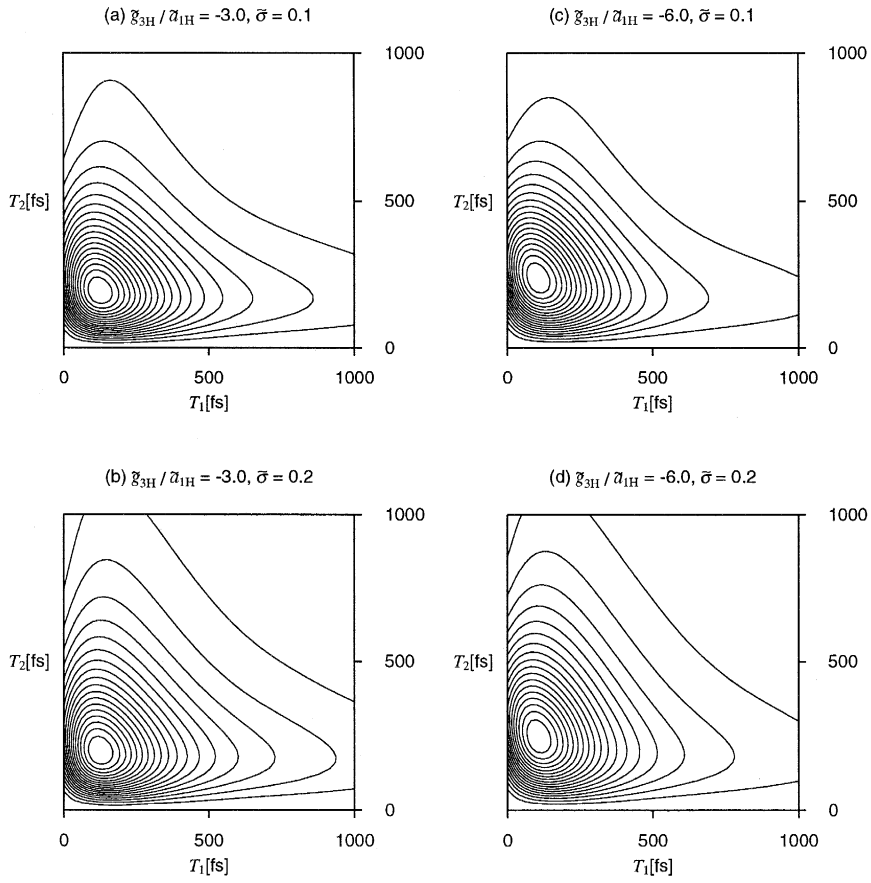

Fig. 4. Inhomogeneous effects in carbon disulfide calculated by using parameters determined from the third-order experiment. The anharmonic parameter $\tilde{g}_{3H}$ is $-3.0\tilde{a}_{1H}$ in (a) and (b) and $-6.0\tilde{a}_{1H}$ in (c) and (d). The inhomogeneous parameter $\tilde{\sigma}$ is 0.1 in (a) and (c) and 0.2 in (b) and (d).

ics can be expected to be homogeneous, since this is a random process. However, at short times the structure of the liquid is essentially fixed so that the librational motion can be influenced by the local structure. To reflect this situation, here, we take into account the inhomogeneous distribution of the frequency Ω_H and thus we have

$$I^{(5)}(T_1,T_2) = \left| \int_0^\infty \frac{\mathrm{d}\,\Omega'_H}{\sqrt{2\pi}\,\sigma} \mathrm{e}^{-(\Omega'_H-\Omega_H)^2/2\sigma^2} \times \left\{ R^{\mathrm{AH}}_{\Omega'_H}(T_1,T_2) + R^{\mathrm{NL}}_{\Omega'_H}(T_1,T_2) \right\} \right|^2, \tag{3.7}$$

where $R^{\mathrm{AH}}_{\Omega'_H}(T_1,T_2)$ and $R^{\mathrm{NL}}_{\Omega'_H}(T_1,T_2)$ are respectively defined by Eq. (3.4) and Eq. (3.5) with Ω_H (in ζ_H) replaced by Ω'_H. In this paper, we do not present the results in the case where anharmonicity of the lower mode is taken into account. This is because in such a case, we could not fit the experimental data [13].

Results of numerical simulations are presented in Fig. 4. The anharmonic parameter is set as $\tilde{g}_{3H}/\tilde{a}_{1H} = -3.0$ in (a) and (b), while it is set as $\tilde{g}_{3H}/\tilde{a}_{1H} = -6.0$ in (c) and (d). From Fig. 4, we see that this inhomogeneity prolongs decay time along both T_1 and T_2 directions. However, decay time in T_2 direction is elongated more than that in T_1 — this tendency becomes notable and thus the two decay times become comparable as the width σ or anharmonicity g_3 gets large. These features are consistent with the result for the single-mode case: if we compare Fig. 2(a) with Fig. 2(c) the tendency of the delocalization is stronger in the T_2 direction than in the T_1 direction. In other words, the decay time in T_2 direction divided by that in T_1 direction gets smaller as the inhomogeneity gets smaller. However, even in the homogeneous limit, T_2 decay time divided by T_1 decay time is larger than the experimental data, as shown in Ref. [13]. Thus, the present analysis indicates that this type of inhomogeneity plays a minor role in CS_2.

4. Discussion

As in the other fifth-order analyses, in this paper, the pulse bandwidth is assumed to be infinitely short compared with slow nuclear dynamics. However, faster intramolecular dynamics has started to be probed through the fifth-order processes by the recently developed heterodyne technique with shorter pulses [10]. As pointed out in Ref. [10], because of the finite pulse bandwidth, the response at small T_1 is a superposition of two responses due to the symmetric nature of the signal. This pulse width convolution effect should be incorporated into theory in order to interpret short-time dynamics of such experimental data obtained with shorter pulses. This is now underway.

Observation of the intramolecular mode, for which the mode of the Brownian model has a clear physical picture such as stretching or bending, has also brought up the problem of coupling between modes. For such weakly damped intramolecular modes, the 2D Fourier transform of the original 2D (time-domain) Raman signal is more suitable for interpretations, and such a frequency domain signal shows the cross peaks, suggesting the existence of the coupling of the modes [10,18]. However, the coupling in the previous theories is limited to the one through polarizability (polarizability-induced coupling). (We note here that this polarizability-induced coupling case has been studied in the molecular dynamics approach [19].) We should compare this coupling effect with the effects of the intrinsic coupling (the coupling through the term in the Hamiltonian), in order to analyze the 2D experimental data in the frequency domain. This is also underway.

In conclusion, we derived an analytical expression of the 2D Raman signal for a multi-mode Brownian oscillator model with taking into account a weak anharmonicity of the potential and inhomogeneity of oscillators. We carried out a model calculation of a simple single-mode case. The numerical results for CS_2 are also obtained by using parameters determined from the third-order experiment and are compared with a fifth-order experiment of CS_2. The result suggests that inhomogeneity is weak in this substance.

Acknowledgements

We would like to thank Dr. Andrei Tokmakoff and Professor Graham R. Fleming for sending some of their results prior to publication.

References

[1] Y. Tanimura, S. Mukamel, J. Chem. Phys. 99 (1993) 9496.
[2] K. Tominaga, K. Yoshihara, Phys. Rev. Lett. 74 (1995) 3061.
[3] K. Tominaga, K. Yoshihara, J. Chem. Phys. 104 (1996) 1159.
[4] K. Tominaga, K. Yoshihara, J. Chem. Phys. 104 (1996) 4419.
[5] K. Tominaga, Off-resonant Fifth and Seventh Order Time-Domain Nonlinear Spectroscopy on Vibrational Dephasing in Liquids, Advances in Multi-photon Processes and Spectroscopy, Vol. 11 (World Scientific, Singapore, 1997, in press).
[6] T. Steffen, K. Duppen, Phys. Rev. Lett. 76 (1996) 1224.
[7] T. Steffen, J.T. Fourkas, K. Duppen, J. Chem. Phys. 105 (1996) 7364.
[8] T. Steffen, K. Duppen, J. Chem. Phys. 106 (1997) 3854.
[9] A. Tokmakoff, G.R. Fleming, J. Chem. Phys. 106 (1997) 2569.
[10] A. Tokmakoff, M.J. Lang, D.S. Larsen, G.R. Fleming, Chem. Phys. Lett. 272 (1997) 48.
[11] V. Khidekel, S. Mukamel, Chem. Phys. Lett. 240 (1995) 304.
[12] V. Khidekel, V. Chernyak, S. Mukamel, J. Chem. Phys. 105 (1996) 8543.
[13] K. Okumura, Y. Tanimura, J. Chem. Phys., in press.
[14] K. Okumura, Y. Tanimura, J. Chem. Phys. 106 (1997) 1687.
[15] K. Okumura, Y. Tanimura, Phys. Rev. E 53 (1996) 214.
[16] K. Okumura, Y. Tanimura, J. Chem. Phys. 105 (1996) 7294.
[17] K. Okumura, Y. Tanimura, Phys. Rev. E, in press.
[18] A. Tokmakoff, private communication; A. Tokmakoff, M.J. Lang, D.S. Larsen, G.R. Fleming, V. Chernyak, S. Mukamel, Two-dimensional Raman Spectroscopy of Vibrational Interactions in Liquids, Phys. Rev. Lett., submitted.
[19] S. Saito, I. Ohmine, private communication.